Nuclear Materials and Energy 26 (2021) 100926

Contents lists available at ScienceDirect

Nuclear Materials and Energy

journal homepage: www.elsevier.com/locate/nme

Towards assessment of plasma edge transport in Neon seeded plasmas in disconnected double null configuration in EAST with SOLPS-ITER

D. Boeyaert [a,c,*], S. Wiesen [a], M. Wischmeier [b], W. Dekeyser [c], S. Carli [c], L. Wang [d], F. Ding [d], K. Li [d], Y. Liang [a,d], M. Baelmans [c], EAST-team [1]

[a] Forschungszentrum Jülich, Institut für Energie- und Klimaforschung - Plasmaphysik, 52425 Jülich, Germany
[b] Max-Planck-Institut für Plasmaphysik, Boltzmannstraße 2, 85748 Garching, Germany
[c] KU Leuven, Department of Mechanical Engineering, Celestijnenlaan 300, 3001 Leuven, Belgium
[d] Institute of Plasma Physics, Chinese Academy of Sciences, Hefei 230031, People's Republic of China

ARTICLE INFO

Keywords:
EAST
Neon seeding
DDN
SOLPS-ITER

ABSTRACT

Energy dissipation in the plasma edge is key for future tokamaks. The potential of neon as radiating seeding species in disconnected double null (DDN) configuration is assessed in EAST discharges in high confinement mode (H-mode). As the separation between the two separatrices in the studied DDN discharges is minimum 1.5 cm, the configuration is effectively a single null configuration, and the benefits of the double null topology are minimal. Neon seeding, on the other hand, has a favourable effect: both the target heat flux and the divertor temperature decrease more than five-fold with increased seeding rate in high-recycling conditions. Interpretive edge plasma simulations with SOLPS-ITER in support of ongoing transport analysis are presented. For the unseeded case the numerical results agree with the experimental data within a factor two for the target temperature conditions and measured neutral pressures in the active divertor. The key for achieving good agreement is a suitable selection of coefficients for anomalous transport and neutral conductances between the upper cryopump and the main chamber.

1. Introduction

Radiation induced energy dissipation in the pedestal and scrape-off layer (SOL), the edge, is key for future fusion devices with a metal wall like ITER and DEMO to solve the challenge of power exhaust [1]. In order to achieve divertor detachment, extrinsic impurity seeding is required. Low-Z impurities or noble gases with a lack of surface chemistry like neon (Ne) are key candidates as main radiator. They can dissipate power through line radiation and thus redistribute the power over a larger area compared to the plasma wetted zone at the divertor targets. Recently, large tokamaks like JET have proven the ability to handle stable H-modes with Ne seeding in a metallic environment [2]. EAST, the only tokamak in the world capable of operating long pulses up to ≈100 s with a partial metallic wall, identified stable Ne-seeded H-mode regimes [3]. In EAST the main, upper divertor is made of tungsten (W) whilst most of the other wall, including the lower divertor, is made of carbon (C).

To leverage dissipation in tokamaks through geometrical redistribution of energy, double null (DN) configurations are a promising alternative to the standard single null (SN) magnetic configuration [4–6]. Whilst decreasing the separation between the separatrices (dr_{sep}), the peak heat flux on the primary divertor targets decreases, and the heat flux to the inner divertor target is significantly reduced, which leads to an increased power load symmetry in the reactor. This is beneficial for improved confinement. As a result, DN is a potential configuration for the European DEMO reactor [7]. In contrast to most (European) tokamaks, EAST has the flexibility to operate both in upper single null (USN) and in DN configurations.

In this paper, both Ne seeding and the disconnected DN (DDN) configuration are analysed for the EAST divertor. Similar experiments have been studied at the DIII-D tokamak by Petrie et al. [8–10] showing a beneficial effect on the peak heat flux reaching the targets. However, in contrast to EAST, DIII-D has a full carbon wall. Due to limitations in heating power at EAST, the leakage of Ne towards the core increased with the amount of Ne whilst performing Ne-seeded H-mode experiments. As a consequence, it was difficult to achieve stable H-mode plasmas and optimise the seeding parameters in EAST. Based on the presented experiments, and by employing an improved understanding

* Corresponding author at: Forschungszentrum Jülich, Institut für Energie- und Klimaforschung - Plasmaphysik, 52425 Jülich, Germany.
E-mail address: d.boeyaert@fz-juelich.de (D. Boeyaert).
[1] See appendix of B.N. Wan et al., Nucl. Fusion 59 (2019) 112003.

https://doi.org/10.1016/j.nme.2021.100926
Received 31 July 2020; Received in revised form 7 January 2021; Accepted 22 January 2021
Available online 27 January 2021

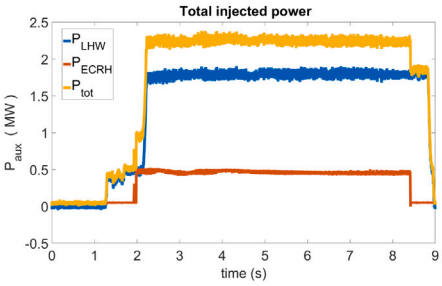

(a) Injected power during the discharges. During all discharges $\sim 2.25\,MW$ of power was applied consisting of $\sim 1.80\,MW$ LHW and $\sim 0.45\,MW$ ECRH.

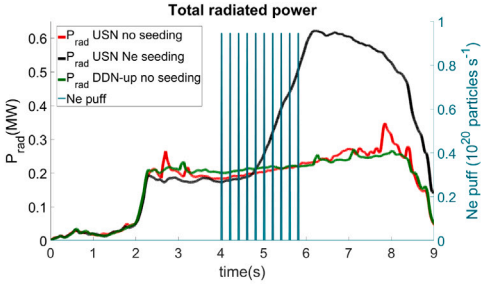

(b) Total radiated power measured with the AXUV system (left axis) and Ne puff (right axis). Ne was puffed in pulses of around 10 ms and located around the strike point at the UOT as indicated in figure 4.

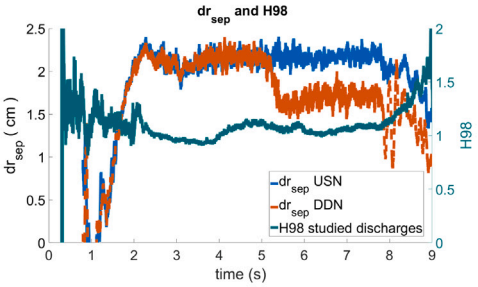

(c) dr_{sep} for the USN and DDN-up discharges (left axis) and a profile of H98 which was similar for all the performed discharges (right axis).

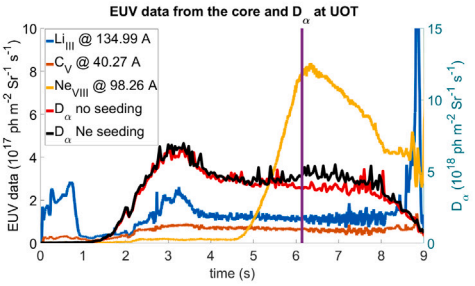

(d) EUV spectroscopy data for main radiators in the core (left axis) and the filterscope data for the observed D_α radiation in the unseeded and Ne-seeded USN discharge measured in the SOL at the UOT (right axis). The Li_{III} and C_V radiation is similar for the seeded and unseeded discharge. The Ne_{VIII} radiation for the seeded discharge is shown. The studied time into the discharge is indicated in purple.

Fig. 1. Overview of the main experimental parameters of the studied discharges through this paper.

of transport through SOLPS-ITER simulations, further optimisation is envisaged also for seeded long pulse operation at EAST in connected DN (CDN) configuration. Special attention is given to anomalous transport in the SOL. The inclusion of drifts is planned for future simulations.

In this paper we focus on USN and DDN experiments in H-mode performed in the EAST experimental campaign of 2019. For the transport analysis, SOLPS-ITER simulations [11,12] have been set up for the USN configuration and the model results are presented in comparison with the experimental data.

2. Description of EAST H-mode Ne-seeded discharges in USN & DDN

In EAST, Ne experiments were performed to study the efficiency of Ne-seeding induced divertor power dissipation. A total heating power of 2.25 MW (1.80 MW Lower Hybrid Wave (LHW) and 0.45 MW Electron Cyclotron Resonance Heating (ECRH)) was applied. The toroidal magnetic field was 2.4 T and the plasma current 400 kA. Deuterium was injected at the outer mid-plane (OMP) in a feedback loop to keep the separatrix electron density constant ($n_{e,sep} \sim 1.0 \cdot 10^{19}$ m^{-3}), whilst Ne was puffed at the strike point in the upper outer target (UOT) as indicated in Section 3 in Fig. 4. The Greenwald fraction was $f_{GW} = \frac{n_{av}}{n_{GW}} \sim 0.6$, with n_{av} the average density and n_{GW} the Greenwald density. An overview of the main discharge parameters is given in Fig. 1.

Three discharges are studied: a reference discharge in an USN configuration, a Ne-seeded discharge in an USN configuration and a non-seeded discharge in a DDN configuration. As the plasma parameters in the non-seeded USN and DDN discharges are similar, the seeded DDN discharge is not discussed here.

USN discharges in EAST were established as DDN configurations with an active upper divertor (DDN-up) with $dr_{sep} \sim 2$ cm. To avoid a power overload on the lower C divertor, only a scan of dr_{sep} from 2 cm to 1.5 cm was possible. Therefore, the discussed DDN experiments are DDN-up experiments with a separation of 1.5 cm.

Ne was injected with 10 pulses of around 10 ms in the discharge as shown in Fig. 1(b). After these 10 pulses, the behaviour of the plasma is studied. The power remained constant throughout the discharge (Fig. 1(a)).

The absolute extreme ultraviolet (AXUV) system of EAST showed that with Ne seeding, the total radiated power increased and saturated at a level of $\sim$ 30% of the total power (Fig. 1(b)). At the UOT, the injected Ne was observed with the divertor spectrometer (not shown). Based on the data from the extreme ultraviolet (EUV) spectrometer, the Ne radiation increased in the core region (Fig. 1(d)): the measured line intensities of the charge states of Ne (Ne_{VII} and Ne_{VIII}) rose by an order of magnitude. This indicates an increased Ne transport from the main SOL into the core region. Independent of the Ne injection rate, line emission of C, W and Li was observed in the core as shown in Fig. 1(d) for C and Li. Also the divertor spectrometer at the UOT indicates a higher concentration of these elements. In the core, especially Li (coming from the Li coating on the wall) was present during all discharges, whilst at the UOT, C was the main impurity source (when there was no Ne puff). The same behaviour was observed during the discharges in USN configuration and in DDN-up configuration. As USN discharges in EAST are in fact DDN-up discharges, it is likely that the observed C came from the lower C divertor. This hypothesis is to be proven by the interpretation of the modelling results as the source of the observed C radiation was not measured.

The EAST Thomson Scattering (TS) system is mainly suited for core profiles, but as some measurement points are lying in the edge region, the edge electron density (n_e) and edge electron temperature (T_e) at the OMP are also obtained (Fig. 2). Based on a fit through the TS data, the upstream decay lengths for temperature and density are estimated:

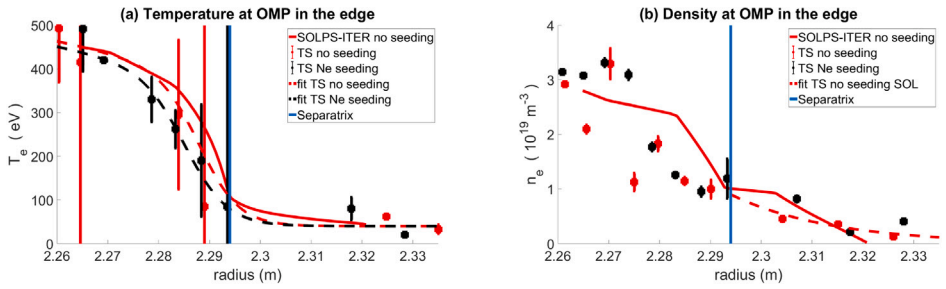

Fig. 2. Radial profiles of the electron temperature (a) and density (b) at the outer midplane, and the predicted profiles in the SOLPS-ITER simulations. The fit through the experimental T_e data is used to estimate $\lambda_{Te} \approx 4.5$ mm. The same procedure results in $\lambda_{ne} \approx 2.0$ cm.

$\lambda_{Te} \approx 4.5$ mm and $\lambda_{ne} \approx 2.0$ cm. The profiles in Fig. 2 indicate a limited influence of Ne seeding on the upstream profiles, but the uncertainty on the experimental data is too large to draw accurate conclusions.

Due to uncertainty in the separatrix position, the profiles were shifted based on an estimate for the OMP separatrix temperature ($T_{e,sep}^{OMP}$). Using the basic two point model [13], $T_{e,sep}^{OMP}$ was found to be between 70 eV and 140 eV. This range of possible outcomes for $T_{e,sep}^{OMP}$ is caused by uncertainties in the two point model assumptions: the sheath transmission coefficient γ, the electron heat conductivity coefficient κ_{0e} and the target electron density $n_{e,t}$. Therefore, $T_{e,sep}^{OMP}$ is assumed to be equal to 100 eV in the non-seeded case. In the Ne-seeded case the spatial distribution of the radiation from AXUV suggests a significant increase in the core radiation due to the Ne seeding. This implies that $T_{e,sep}^{OMP}$ will be lower. Due to the uncertainties on the T_e data from the TS system, this difference cannot be quantified accurately. Therefore, the $T_{e,sep}^{OMP}$ should be further investigated with SOLPS-ITER simulations of the Ne-seeded case.

The Divertor Langmuir Prove (DivLP) system at EAST consists of a set of triple probes. As there is no ELM-filtering available at EAST, the median of five time slots around the studied time instant is taken to lower the influence of ELMs on the plasma parameters as much as possible. Due to the long pulses performed earlier at EAST, the effective area of some probe tips (A_{pr}) was modified and is not known exactly anymore. The data affected by this change have been excluded from the analysis. For the T_e, n_e and the heat flux (q_t), additional measurement points have been excluded as they rely on the less accurate voltage measurements.

Fig. 3 compares parallel j_{sat} 3(a), T_e 3(b) and perpendicular q_t 3(c) at the UOT for the three discharges. In contrast to j_{sat} and T_e, q_t is not measured directly but derived from the two previous values: $q_t = \gamma T_e j_{sat} e^{-1} \sin(\theta)$ with $\gamma = \gamma_i + \gamma_e \sim 7$ the total sheath heat transmission coefficient, e the charge of a singly ionised ion and $\theta \sim 1°$ the incidence angle of the magnetic field [14]. This calculation is an approximation for the heat flux towards the targets.

Ne seeding reduced T_e and q_t in the DivLP profiles (Fig. 3). However, Ne did not drive the divertor into full detachment (for the definition of full detachment and the subcategories of detachment, the terminology of Ref. [15] is used). Based on the T_e and q_t profiles (Figs. 3(b) and 3(c)), the discharge was in energy detachment. j_{sat} (Fig. 3(a)), on the other hand, increased up to ~25% due to the added Ne. This indicates that no significant decrease of ion flux towards the divertor target took place, signifying momentum losses required for momentum detachment. In order to achieve particle detachment, an increased plasma recombination is anticipated at $T_e < 5$ eV. Fig. 1(d) shows the D_α signal from the filterscope a few cm away from the strike point at the UOT in the SOL. A small increase of the D_α emission was observed. As no information about the D_γ or the Ly_β ratios is available, no conclusion about particle detachment can be made based on the measured change in D_α emission [16–18]. As momentum detachment is not reached, full detachment does not take place and the discharge is in the high recycling regime (HRR) [13] with the low field side (LFS) divertor dissipating power via radiation.

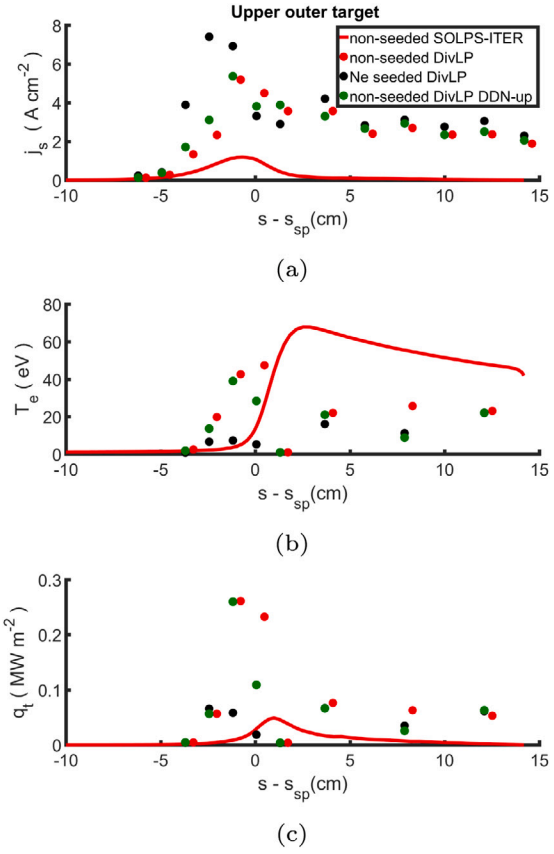

Fig. 3. Radial profiles at the UOT of the saturation current (a), the electron temperature (b) and the parallel heath flux (c) as function of the distance to the separatrix position (in cm). The data of the DivLP system are shown together with the predictions of the SOLPS-ITER simulations. For the DivLP data a comparison between the USN and DDN-up data is given. The studied time into the discharge was at 6.15 s and therefore the average from the experimental data at 6.05, 6.10, 6.15, 6.20 and 6.25 s was taken.

The difference between the radiated power in the USN configuration and in the DDN-up configuration is negligible (see Fig. 1(b)). The DivLP data of Fig. 3 confirm that there is no significant difference. Therefore, it is concluded that a separation of 1.5 cm is too large to have any impact on the exhaust regime. This is in agreement with previous work at other devices [5,6] and can be explained by a power decay length being much smaller then 1.5 cm. Based on the TS data, $\lambda_{Te,u}$ is calculated as indicated in Fig. 2. As the Ne-seeded discharge is in the HRR, $\lambda_{q\|} \approx \frac{2}{7}\lambda_{Te,u} \approx 1.3$ mm [13]. For the unseeded case, as $\frac{T_{e,u}}{T_{e,t}} \approx 1.6$, the formulas for the sheath-limited regime are used which results in $\lambda_{q\|} \approx \left(\lambda_{ne,u}^{-1} + \frac{3}{2}\lambda_{Te,u}^{-1}\right)^{-1} \approx 2.6$ mm.

The issue with the calculated $\lambda_{Te,u}$ and $\lambda_{ne,u}$ is the quality of the TS data. Therefore, λ_q is also estimated with the formula of Eich et al. [19]:

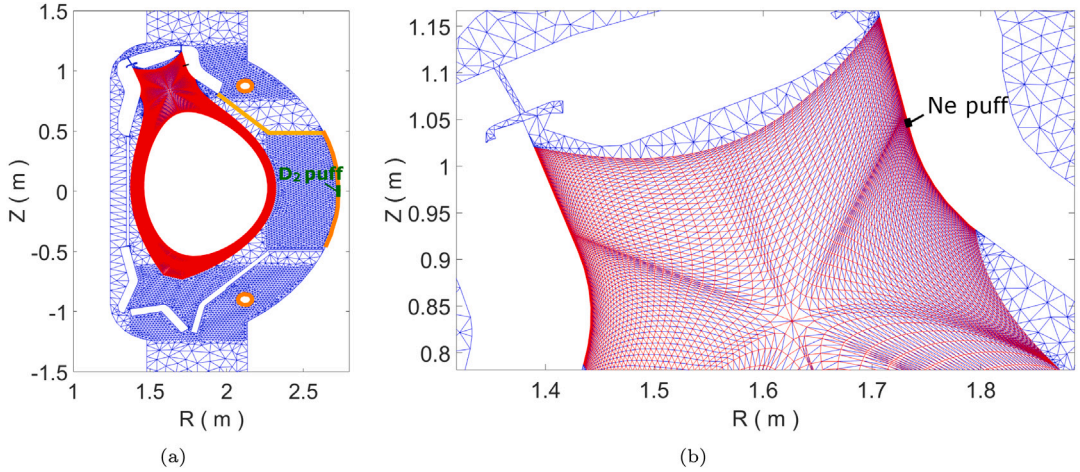

Fig. 4. Overview of the SOLPS-ITER grid (a) and a zoom around the X-point and the divertor targets (b). The red grid is the B2.5 grid and the blue grid is the EIRENE grid. The pumps are indicated in orange, the D2 puffing location in green, the Ne puffing location in black and the 10% transparent surfaces in yellow. (For interpretation of the references to colour in this figure legend, the reader is referred to the web version of this article.)

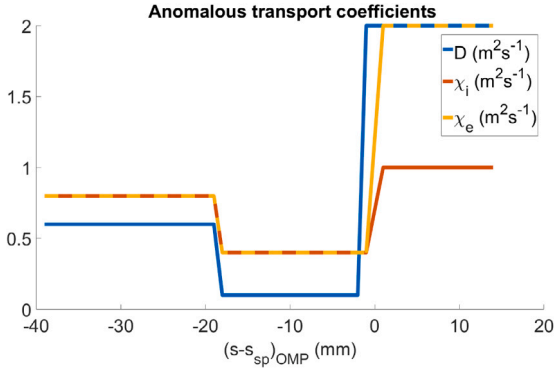

Fig. 5. Used profiles for the radial transport coefficients.

$\lambda_{q\|} \approx (0.63 \pm 0.08) \cdot B_{pol,OMP}^{-1.19\pm0.08} \approx 5$ mm which also concludes that dr_{sep} should be smaller to benefit from the DDN-up configuration.

As indicated in Fig. 1(b), the radiated power observed by the AXUV system was approximately 0.6 MW. As the AXUV system only covers the core region, this power was radiated core power (P_{rad}). Based on the Martin scaling [20], a minimum power to maintain H-mode (P_{LH}) of 1.6 MW is required. In the studied discharge the difference between $P_{loss} = P_{heat} - P_{rad}$ and P_{HL} was small. Therefore, discharges with stronger Ne injection (and so a higher P_{loss}) could not be kept in H-mode confinement and an H-L back transition took place.

3. Initial SOLPS-ITER transport assessment

As the experimental results suggested no significant difference between the reference USN discharge and the non-seeded DDN-up discharge, the main focus is on modelling the unseeded reference discharges in USN using the SOLPS-ITER code. The simulations with seeded Ne will be presented in a later publication.

The created USN grid including the pumping and puffing locations is depicted in Fig. 4. In order to guarantee numerical stability, it is important that the size of neighbouring plasma grid cells does not differ too much and that large cells are only present in regions of shallow gradients of the plasma parameters. This results in three main requirements: a symmetric grid around the X-point, smooth transitions between the different grid cells and small grid cells at the divertor targets. For the USN grid these conditions are fulfilled in the 155×70 grid as shown in Fig. 4. The radial mesh width between the separatrix and the SOL boundary at the OMP is about 2.5 cm. This grid is marginally wide which could give rise to additional, artificial ionisation sources inside the separatrix. In order to verify this, it will be studied in future simulations if a DDN-up grid with larger SOL width produces a similar outcome.

In the presented simulations, only deuterium is included as species in the plasma and drifts are not taken into account. On the core boundary of the grid, the boundary conditions (BC) are of Dirichlet type: a constant electron temperature ($T_e = T_i = 450$ eV) and a constant electron density ($n_e = 2.8 \cdot 10^{19}\ m^{-3}$) (c.f. Fig. 2). The energy crossing the core boundary is in agreement with the experimental $P_{in} - P_{rad} \approx 2.0$ MW, as an energy balance for the performed simulations results in ~ 1.9 MW crossing the core boundary. A Bohm–Chodura BC is applied at the targets for all conservation equations. At the boundary to the private flux zone and the radially outermost SOL boundary, a leakage BC is imposed for continuity (leakage factor of $-1.0 \cdot 10^{-2}$) and energy conservation (leakage factor of $-1.0 \cdot 10^{-2}$ for the ions and $-1.0 \cdot 10^{-4}$ for the electrons), and a zero gradient BC for momentum.

Deuterium molecules and atoms are modelled kinetically using EIRENE [21]. The main pumping areas are assumed to be the upper cryopump (pumping albedo $\sim$ 0.939), the lower cryopump (albedo $\sim$ 0.941) and the turbopump at the outer midplane (albedo $\sim$ 0.991). Chemical and physical sputtering as well as recycling at walls other than the pumps are not taken into account for any species. The neutral model and reactions used in the simulations can be found in [22].

The two remaining important input parameters for the simulations are the ad-hoc anomalous transport coefficients and the neutral conductances (the extra structures in the EIRENE grid to match the neutral pressures). For the anomalous transport parameters for H-mode discharges, a non-constant radial profile for diffusion including a transport barrier is assumed (as for instance in [23]).

As the simulations are single-fluid simulations with only deuterium, the influence of the lower C divertor is ignored. As discussed in Section 2, carbon is observed during the discharge and it will be taken into account in future simulations. The present simulations are considered to be converged when the main plasma parameters (T_e, n_e and the neutral pressure) do not change anymore for at least 0.15 s of plasma time.

In Figs. 2 and 3 the comparison between the simulations and the experiments is shown. The first aim is to match the experimental profiles of the modelled EAST discharge, starting with n_e and T_e profiles at the OMP. The initial anomalous transport coefficients were iterated until agreement was found (Fig. 2). The corresponding coefficients are given in Fig. 5. The simulation results for the upstream n_e profile show a change in slope at $R = 2.30$ m which is absent in the experimental

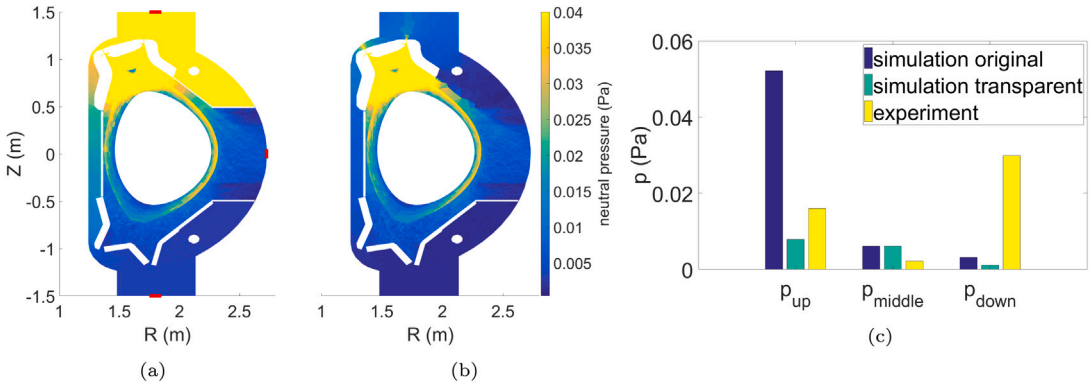

Fig. 6. Pressures obtained with SOLPS-ITER simulations. In (a) the simulated pressures without any modifications to the structure are shown, in (b) the ones with the 10% transparent structure indicated in Fig. 4 and in (c) a comparison is given between the experiments and the simulations. The locations of the pressure gauges are indicated in red in the left figure. The upper and lower pressure gauges are further away from the main vessel as indicated in the paragraph below. (For interpretation of the references to colour in this figure legend, the reader is referred to the web version of this article.)

data. As there is no feature in the simulation setup other then the transport parameters which can cause this change in slope, a further improvement of the transport parameters is planned. Another way to study the agreement for the upstream parameter is the comparison of the power scrape-off width λ_q. For the simulations $\lambda_q = 10$ mm, which is a factor two higher than the one predicted by the Eich-scaling and nearly four times as high as the one calculated from the TS data. The deduced transport coefficients will likely be different when drifts are activated in future simulations.

As indicated in Fig. 3 agreement between the measurements and SOLPS-ITER predictions at the UOT is limited. T_e agrees within a factor of two and the predicted peak in the j_{sat} profile, is a factor of five lower than measured. As the q_t profile is calculated in a similar way as the experimental profile, the predicted q_t profile is a factor ten smaller than measured. As drifts are not included in the current simulations, it will be investigated if including these terms will improve the downstream agreement.

As demonstrated by Kallenbach et al. in [24], predicting the neutral pressures with SOLPS-ITER can help in a later step to give a correct interpretation to the measured plasma parameters. Therefore, it is aimed to match the neutral pressure at EAST at the three available pressure gauges: one at 3.0 m below the vessel, one at 2.5 m above the vessel and one at the vessel wall around the OMP (see Fig. 6).

In [25] it is shown that, in order to match these pressures, neutral conductances are required in the SOLPS-ITER simulations. These conductances identify the paths which the neutrals can follow [26] and are for the first time studied for EAST. To identify the neutral paths, a visual analysis of the inside of EAST suggests that most toroidal gaps are located between the end of the UOT plate and the vessel wall (yellow line in Fig. 4). A new simulation in which this structure is made 10% transparent shows that the agreement with uppermost experimental pressure measurements improves, keeping the energy balance at the core boundary unchanged (Fig. 6(c)). However, the agreement with the middle pressure gauge, seems not to change due to the added conductances and the agreement for the lower pressure gauge even decreases. On the other hand, the plasma profiles at the OMP and targets are not affected significantly and the ion and atomic throughput across the core boundary do not change.

4. Summary

In order to reduce the peak loads in the particle and power exhaust, Ne seeding experiments were carried out at EAST in USN and DDN-up configuration.

Ne seeding increased the level of dissipation in the EAST low field side (LFS) USN divertor and leads to a high-recycling regime with a clear signature of energy detachment at the highest achieved Ne seeding levels whilst keeping H-mode confinement. However, it was not possible to increase further Ne injection to drive the LFS divertor into a fully detached regime due to a lack of power to maintain H-mode confinement. It remains to be proven that at EAST, with higher heating power above the H-L back transition threshold, the compression of Ne at least saturates to effectively dissipate energy inside the divertor similar to recent JET studies [2].

The impact of the studied DDN-up configuration on the particle and heath fluxes reaching the divertor targets was hampered by a too large separation of 15 mm between the separatrices. Hence, a beneficial effect towards power load distribution in comparison with an USN configuration is yet to be proven at lower dr_{sep} below $\lambda_q \approx 1.3 - 5$ mm. Unfortunately, EAST could not be operated closer to real (connected) DN scenario as the interaction with the lower carbon divertor impacted the stabilisation of the discharge even further.

Initial SOLPS-ITER simulations have been carried out to study the transport mechanisms of the plasma particles behind the observed changes in plasma behaviour. The main focus is on finding the radial transport coefficients and the neutral conductances. The upstream T_e profile in the current simulations agrees well with the experimental profiles whilst the upstream n_e profile still needs to be improved. Additionally, comparison with the UOT data shows that the SOLPS-ITER results are at least a factor two off the experimental data. Further modifications in the transport coefficients and inclusion of drifts are planned to improve the agreement. In the current simulations a first step towards the matching of the neutral pressures in the EAST upper divertor is taken by studying the impact of reducing the conductance between the main and the pumping chambers, showing that this reduction leads to a better agreement with the pressure measurements.

CRediT authorship contribution statement

D. Boeyaert: Conceptualization, Methodology, Software, Validation, Formal analysis, Investigation, Data curation, Writing - original draft. **S. Wiesen:** Conceptualization, Methodology, Software, Validation, Project administration, Writing - review & editing, Funding acquisition, Supervision. **M. Wischmeier:** Conceptualization, Project administration, Funding acquisition, Supervision. **W. Dekeyser:** Methodology, Software, Validation, Data curation, Writing - review & editing. **S. Carli:** Methodology, Software, Validation, Data curation, Writing - review & editing. **L. Wang:** Investigation, Resources. **F. Ding:** Investigation, Resources. **K. Li:** Investigation, Data curation, Writing - review & editing. **Y. Liang:** Investigation, Data curation, Resources. **M. Baelmans:** Conceptualization, Supervision.

Declaration of competing interest

The authors declare that they have no known competing financial interests or personal relationships that could have appeared to influence the work reported in this paper.

Acknowledgements

This work has been carried out within the framework of the EUROfusion Consortium and has received funding from the Euratom research and training program 2014–2018 and 2019–2020 under grant agreement No 633053. The views and opinions expressed herein do not necessarily reflect those of the European Commission.

The SOLPS-ITER simulations were performed at the Marconi supercomputer from the National Supercomputing Consortium CINECA.

References

[1] S. Wiesen, et al., Nucl. Mater. Energy 12 (2017) 3.
[2] S. Glöggler, et al., Nucl. Fusion 59 (2019) 126031.
[3] G.S. Xu, et al., Nucl. Fusion 60 (2020) 086001.
[4] A. Herrmann, Plasma Phys. Control. Fusion 44 (2002) 883.
[5] H. Meyer, et al., Nucl. Fusion 46 (2006) 64.
[6] D. Brunner, et al., Nucl. Fusion 58 (2018) 076010.
[7] R. Ambrosino, et al., Fusion Eng. Des. 146 (2019) 2717.
[8] T.W. Petrie, et al., Nucl. Fusion 48 (2008) 045010.
[9] T.W. Petrie, et al., J. Nucl. Mater. 463 (2015) 1225–1228.
[10] T.W. Petrie, et al., Nucl. Mater. Energy 19 (2019) 267–272.
[11] S. Wiesen, et al., J. Nucl. Mater. 463 (2015) 480.
[12] X. Bonnin, et al., Plasma Fusion Res. 11 (2016) 1403102.
[13] P.C. Stangeby, The Plasma Boundary of Magnetic Fusion Devices, CRC Press, 2000.
[14] J.C. Xu, et al., Rev. Sci. Instrum. 87 (2016) 083504.
[15] A.W. Leonard, Plasma Phys. Control. Fusion 60 (2018) 0044001.
[16] J.L. Terry, et al., J. Nucl. Mater. 266 (1999) 30–36.
[17] D. Lumma, et al., Phys. Plasmas 4 (1997) 2555.
[18] G. McCracken, et al., Nucl. Fusion 38 (1998) 619.
[19] T. Eich, et al., Nucl. Fusion 53 (2013) 093031.
[20] Y. Martin, et al., J. Phys. Conf. Ser. 123 (2008) 012033.
[21] D. Reiter, et al., Fusion Sci. Technol. 47 (2) (2005) 172–186.
[22] V. Kotov, et al., Plasma Phys. Control. Fusion 50 (2008) 105012.
[23] E. Sytova, et al., Nucl. Mater. Energy 19 (2019) 72.
[24] A. Kallenbach, et al., Plasma Phys. Control. Fusion 60 (2018) 045006.
[25] S. Wiesen, et al., 46th EPS Conference on Plasma Physics, 2019, p. I4.103.
[26] W. Dekeyser, et al., Nucl. Mater. Energy 12 (2017) 899.